# INITIAL ASSESSMENT OF RADIATION BEHAVIOR OF VERY-HIGH-DENSITY LOW-ENRICHED-URANIUM FUELS*

G. L. HOFMAN, M. K. MEYER, J. L. SNELGROVE
M. L. DIETZ, R. V. STRAIN, and K-H. KIM*
Argonne National Laboratory
9700 South Cass Avenue
Argonne, Illinois 60439-4815 U.S.A.

*Korea Atomic Energy Research Institute
150, Dukjin-Dong, Yusong-Ku, Taejon, 305-353, Korea

Paper submitted for presentation and
publication in the proceedings of the
1999 International Meeting on
Reduced Enrichment for Research and Test Reactors (RERTR)
Budapest, Hungary
October 3-8, 1999



*Work supported by the U.S. Department of Energy, Office of Nonproliferation and National Security, under Contract No. W-31-109-ENG-38

# INITIAL ASSESMENT OF RADIATION BEHAVIOR OF VERY-HIGH-DENSITY LOW-ENRICHED-URANIUM FUELS*

G. L. HOFMAN, M. K. MEYER, J. L. SNELGROVE
M. L. DIETZ, R. V. STRAIN, and K-H. KIM*
Argonne National Laboratory
9700 South Cass Avenue
Argonne, Illinois 60439-4815 U.S.A.

*Korea Atomic Energy Research Institute
150, Dukjin-Dong, Yusong-Ku, Taejon, 305-353, Korea

## ABSTRACT

Results from the postirradiation examinations of microplates irradiated in the RERTR-1 and -2 experiments in the ATR have shown several binary and ternary U-Mo alloys to be promising candidates for use in aluminum-based dispersion fuels with uranium densities up to 8 to 9 g/cm$^3$. Ternary alloys of uranium, niobium, and zirconium performed poorly, however, both in terms of fuel/matrix reaction and fission-gas-bubble behavior, and have been dropped from further study. Since irradiation temperatures achieved in the present experiments (approximately 70°C) are considerably lower than might be experienced in a high-performance reactor, a new experiment is being planned with beginning-of-cycle temperatures greater than 200°C in 8-g U/cm$^3$ fuel.

## 1. Introduction

Small dispersion fuel plates containing U-10Mo, U-8Mo, U-6Mo, U-4Mo, U-6Mo-1Pt, U-6Mo-0.6Ru, U-10Mo-0.05Sn, U-9Nb-4Zr, U-6Nb-4Zr, U-5Nb-3Zr, $U_2Mo$, and $U_3Si_2$ were irradiated in the Advanced Test Reactor (ATR) to screen their behavior. (The number preceding the alloying element signifies its content in weight percent.) The $U_3Si_2$ samples provided normalization to previous results; the $U_2Mo$ samples were irradiated since $\gamma$-U decomposes into $\alpha$-U plus $U_2Mo$. In addition to machined or ground powders of all alloys, powders of U-10Mo and $U_3Si_2$ produced by centrifugal atomization were provided by the Korea Atomic Energy Research Institute (KAERI). In this paper we summarize the results of these experiments obtained to date (September 1999. A more quantitative analysis of the postirradiation data is presented elsewhere in these proceedings.[1]

## 2. Experiment Description

We have called the fuel plates fabricated for these experiments “microplates” owing to their small size. Their external dimensions are 76 mm x 22 mm x 1.3 mm. The fuel zone is elliptical in shape with major and minor axes of approximately 51 mm and 9.5 mm, respectively; the fuel zone thickness is nominally 0.5 mm. In spite of their small size, we have shown by mechanical analysis that the fuel zone of a microplate is essentially unrestrained in the thickness direction and, consequently, behaves in the same manner as a larger plate. Since the goal of these experiments was to determine as quickly as possible basic information of fuel/matrix interaction and fuel particle swelling, we chose to fabricate plates at about one-half of the goal density in order to ease fabrication problems. The plates were produced by standard powder metallurgy and hot roll-bonding techniques. Although we planned a 25-vol% loading, actual loadings (determined by X-ray density measurements) fell between 26 and 41 vol.%, with an

average of approximately 30 vol.%. The enrichment ranged between 19.1 and 19.8%, and a microplate typically contained about 0.11 g of $^{235}U$.

The irradiation vehicles, designated RERTR-1 and RERTR-2, each consisted of a flow-through "basket" holding eight vertically stacked flow-through capsules. Each capsule held four microplates in a miniature fuel element configuration. The irradiation vehicles occupied small I-hole positions (I-22 and I-23) in the control drum region of the ATR. Based on calculations, the neutron flux, microplate power, surface heat flux, and fuel centerline temperature were approximately $1.3 \times 10^{18}$ n $m^{-2}$ $s^{-1}$, 500 kW, $5.5 \times 10^{5}$ W $m^{-2}$, and 70°C, respectively, at the axial position of highest neutron flux at the start of the irradiation. Vehicle RERTR-1 was irradiated for 94 effective full-power days (EFPD) during the period August 23, 1997, through November 30, 1997, and RERTR-2 was irradiated for 232 EFPD during the period August 23, 1997 through July 6, 1998, achieving (calculated) $^{235}U$ burnups between 39 and 45% and between 65 and 71%, respectively. Experimental particulars for the individual microplates are listed in Table I and II.

TABLE I. Microplate Description and Burnup Data for RERTR-1

| Capsule Position | Microplate Serial No. | Fuel Phase Composition* | Alloy U-Density ($g/cm^3$) | Meat U-Density ($g/cm^3$) | Fuel Burnup (at.%/$U^{235}$) | Fuel Fission Density ($10^{21}$ fissions/$cm^3$) |
|---|---|---|---|---|---|---|
| A-1 | U001 | $U_3Si_2$ | 11.3 | 2.8 | 40 | 2.3 |
| A-2 | T001 | $U_2Mo$ | 13.8 | 3.5 | 40 | 2.8 |
| A-3 | F001 | U-6Nb-4Zr | 14.8 | 3.7 | 40 | 3.0 |
| A-4 | I004 | U-5Nb-3Zr | 15.5 | 3.9 | 40 | 3.2 |
| B-1 | C001 | U-6Mo | 16.7 | 4.2 | 41 | 3.5 |
| B-2 | N002 | U-6Mo-1Pt | 16.5 | 4.1 | 40 | 3.4 |
| B-3 | A001 | U-10Mo | 15.3 | 3.8 | 41 | 3.2 |
| B-4 | M001 | U-6Mo-0.6Ru | 16.5 | 4.1 | 42 | 3.6 |
| C-1 | U003 | $U_3Si_2$ | 11.3 | 2.8 | 43 | 2.5 |
| C-2 | W001 | $U_3Si_2$** | 11.3 | 2.8 | 42 | 2.4 |
| C-3 | D002 | U-4Mo | 17.4 | 4.3 | 42 | 3.7 |
| C-4 | A002 | U-10Mo | 15.3 | 3.8 | 43 | 3.4 |
| D-1 | A006 | U-10Mo | 15.3 | 3.8 | 44 | 3.4 |
| D-2 | P003 | U-10Mo-0.5Sn | 15.3 | 3.8 | 43 | 3.4 |
| D-3 | J001 | U-9Nb-3Zr | 14.2 | 3.5 | 45 | 3.3 |
| D-4 | B001 | U-8Mo | 16.0 | 4.0 | 43 | 3.5 |
| E-1 | C004 | U-6Mo | 16.7 | 4.2 | 43 | 3.7 |
| E-2 | N003 | U-6Mo-1Pt | 16.5 | 4.1 | 43 | 3.6 |
| E-3 | J002 | U-10Mo** | 14.2 | 3.5 | 44 | 3.2 |
| E-4 | B002 | U-6Mo-0.6Ru | 16.0 | 4.0 | 43 | 3.5 |
| F-1 | A007 | U-10Mo | 15.3 | 3.8 | 40 | 3.1 |
| F-2 | P002 | U-10Mo-0.05Sn | 15.3 | 3.8 | 41 | 3.2 |
| F-3 | V001 | U-10Mo** | 15.3 | 3.8 | 42 | 3.3 |
| F-4 | M002 | U-6Mo-0.6Ru | 16.5 | 4.1 | 43 | 3.6 |
| G-1 | F002 | U-6Nb-4Zr | 14.8 | 3.7 | 42 | 3.2 |
| G-2 | I005 | U-5Nb-3Zr | 15.5 | 3.9 | 41 | 3.3 |
| G-3 | T002 | $U_2Mo$ | 13.8 | 3.5 | 41 | 2.9 |
| G-4 | A008 | U-10Mo | 15.3 | 3.8 | 42 | 3.3 |
| H-1 | D004 | U-4Mo | 17.4 | 4.3 | 39 | 3.5 |
| H-2 | W002 | $U_3Si_2$** | 11.3 | 2.8 | 43 | 2.3 |
| H-3 | V002 | U-10Mo** | 15.3 | 3.8 | 39 | 3.1 |
| H-4 | A003 | U-10Mo | 15.3 | 3.8 | 40 | 3.1 |

*Nominal alloy compositions given in wt.%.

**Atomized alloy powder.

TABLE II. Microplate Description and Burnup Data for RERTR-2

| Capsule Position | Microplate Serial No. | Fuel Phase Composition* | Alloy U-Density ($g/cm^3$) | Meat U-Density ($g/cm^3$) | Fuel Burnup (at.%/$U^{235}$) | Fuel Fission Density ($10^{21}$ fissions/$cm^3$) |
|---|---|---|---|---|---|---|
| Z-1 | U004 | $U_3Si_2$ | 11.3 | 2.8 | 66 | 3.8 |
| Z-2 | T003 | $U_2Mo$ | 13.8 | 3.5 | 65 | 4.6 |
| Z-3 | F003 | U-6Nb-4Zr | 14.8 | 3.7 | 66 | 5.0 |
| Z-4 | N001 | U-6Mo-1Pt | 16.5 | 4.1 | 67 | 5.7 |
| Y-1 | C002 | U-6Mo | 16.7 | 4.2 | 68 | 5.8 |
| Y-2 | N004 | U-6Mo-1Pt | 16.5 | 4.1 | 68 | 5.7 |
| Y-3 | A004 | U-10Mo | 15.3 | 3.8 | 68 | 5.3 |
| Y-4 | M003 | U-6Mo-0.6Ru | 16.5 | 4.1 | 68 | 5.7 |
| X-1 | U005 | $U_3Si_2$ | 11.3 | 2.8 | 70 | 4.1 |
| X-2 | W003 | $U_3Si_2$** | 11.3 | 2.8 | 70 | 4.1 |
| X-3 | P004 | U-10Mo-0.05Sn | 15.3 | 3.8 | 68 | 5.3 |
| X-4 | M004 | U-U-6Mo-0.6Ru | 16.5 | 4.1 | 69 | 5.8 |
| W-1 | A009 | U-10Mo | 15.3 | 3.8 | 71 | 5.6 |
| W-2 | P001 | U-10Mo-0.5Sn | 15.3 | 3.8 | 70 | 5.5 |
| W-3 | J003 | U-9Nb-3Zr | 14.2 | 3.5 | 71 | 5.1 |
| W-4 | B003 | U-8Mo | 16.0 | 4.0 | 71 | 5.8 |
| V-1 | C003 | U-6Mo | 16.7 | 4.2 | 67 | 5.7 |
| V-2 | N005 | U-6Mo-1Pt | 16.5 | 4.1 | 68 | 5.7 |
| V-3 | J004 | u-9Nb-3Zr | 14.2 | 3.5 | 68 | 4.9 |
| V-4 | B004 | U-8Mo | 16.0 | 4.0 | 70 | 5.7 |
| U-1 | A010 | U-10Mo | 15.3 | 3.8 | 70 | 5.5 |
| U-2 | P005 | U-10Mo-0.05Sn | 15.3 | 3.8 | 70 | 5.5 |
| U-3 | V003 | U-10Mo** | 15.3 | 3.8 | 70 | 5.5 |
| U-4 | M005 | U-6Mo-0.6Ru | 16.5 | 4.1 | 71 | 6.0 |
| T-1 | F005 | U-6Nb-4Zr | 14.8 | 3.7 | 70 | 5.3 |
| T-2 | C005 | U-6Mo | 16.7 | 4.2 | 69 | 5.9 |
| T-3 | T004 | $U_2Mo$ | 13.8 | 3.5 | 68 | 4.8 |
| T-4 | B005 | U-8Mo | 16.0 | 4.0 | 69 | 5.7 |
| S-1 | D005 | U-4Mo | 17.4 | 4.3 | 69 | 6.2 |
| S-2 | W004 | $U_3Si_2$** | 11.3 | 2.8 | 68 | 3.9 |
| S-3 | V004 | U-10Mo** | 15.3 | 3.8 | 67 | 5.3 |
| S-4 | A005 | U-10Mo | 15.3 | 3.8 | 69 | 5.4 |

*Nominal alloy compositions given in wt.%.

**Atomized alloy powder.

## 3. Experiment Results and Discussion

Considerable information about the extent of the fuel/matrix reaction was derived during fabrication. One of the fabrication steps is a one-hour blister anneal at 485°C. Plate thickness measurements taken before and after the anneal revealed significant thickness increases in all of the U-Nb-Zr plates and in the U-4Mo plates, indicating reaction to form less-dense compounds. As the alloying addition and, hence, the gamma stability decreased, the reaction became more pronounced. The binary U-Mo alloys with at least 6 wt.% Mo and the ternary U-Mo alloys showed little or no thickness increase. More recently, X-ray diffraction was used to study the phase composition of fuel particles removed from fabricated fuel plates. Except for the U-10Mo atomized powder, all of the powders examined contained a significant amount of $\alpha$-U, which must have come from partial decomposition of the $\gamma$-U phase during fabrication. This will be addressed further when the results of the metallography are discussed.

After irradiation and cooling, the capsules were removed from the baskets and shipped to the Alpha-Gamma Hot Cell Facility (AGHCF) at ANL's site in Illinois. Examinations have included visual inspection, thickness measurements, gamma scanning, and metallography. All examinations but the

metallography have been completed. Visual inspection revealed significant corrosion of the cladding surface, especially over the fuel zone. Cladding breaches, subsequently shown to be due to pitting corrosion, were identified in five microplates. This is a common problem in the ATR environment and is not related to fuel performance. Thickness measurements on the RERTR-1 plates showed, in general, decreased thickness over the fuel zone, consistent with erosion or spallation of a corrosion product. The plates from RERTR-2, on the other hand, increased modestly in thickness over the fuel zone, consistent with swelling observed during metallographic examination. Samples from several microplates have been submitted for burnup analysis. We also plan to perform a standard postirradiation blister anneal test on selected microplates.

The most-important information has come from optical metallography of ground and polished sections and, especially, from scanning electron microscopy (SEM) of fracture surfaces of fuel particles as well as of polished samples.

### 3.1 RERTR-1 @ ~40% U-235 Burnup

Optical metallography of U-10 Mo samples is shown in Fig. 1. The microstructure has not noticeably changed after this burnup interval. There are no fission gas bubbles visible at this 500x magnification, and fuel-Al interaction is barely discernable. SEM fractographs shown in Fig. 2 reveal the extent of fission gas bubble formation as well as the depth of the fuel-Al interfiffusion layer at the particle surface. The fission gas bubbles have primarily formed at the boundaries between the small grains of the rapidly solidified atomized fuel particles. It is entirely consistent with the general observation that grain boundaries are the preferred site for fission gas bubble nucleation and growth, particularly at lower irradiation temperatures.

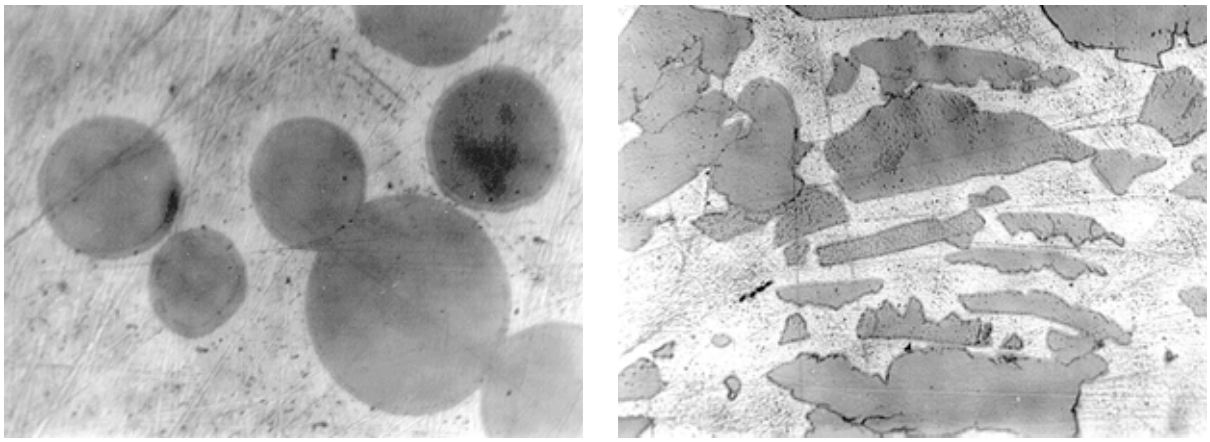

Fig. 1. As-polished cross-section of atomized and ground U-10Mo samples after ~40 at% U-235 burnup.

There are apparent similarities, as well as some differences, to be noted in comparing the atomized and ground fuel samples. The fuel-Al interaction layer, when measured on several fuel particles, is identical in width and appearance. In the ground fuel, fission gas bubbles have also, in general, formed on what appear to be grain boundaries. However, in a substantial fraction of the ground fuel particles, a more profuse bubble population with larger diameters was found. The overall bubble volume fraction, however, is relatively small for both atomized and ground fuel, signifying low fuel swelling at 40% burnup. A determination of the magnitude of swelling awaits quantitative analysis of the bubble distributions. Regarding the above noted similarities and differences between the two fuels the following, preliminary, explanation is offered: the fission gas bubble morphology in the atomized fuel may be called "classic" in so far the bubbles nucleated and grew first on preexisting grain boundaries that resulted from the fine grain structure formed during atomization.

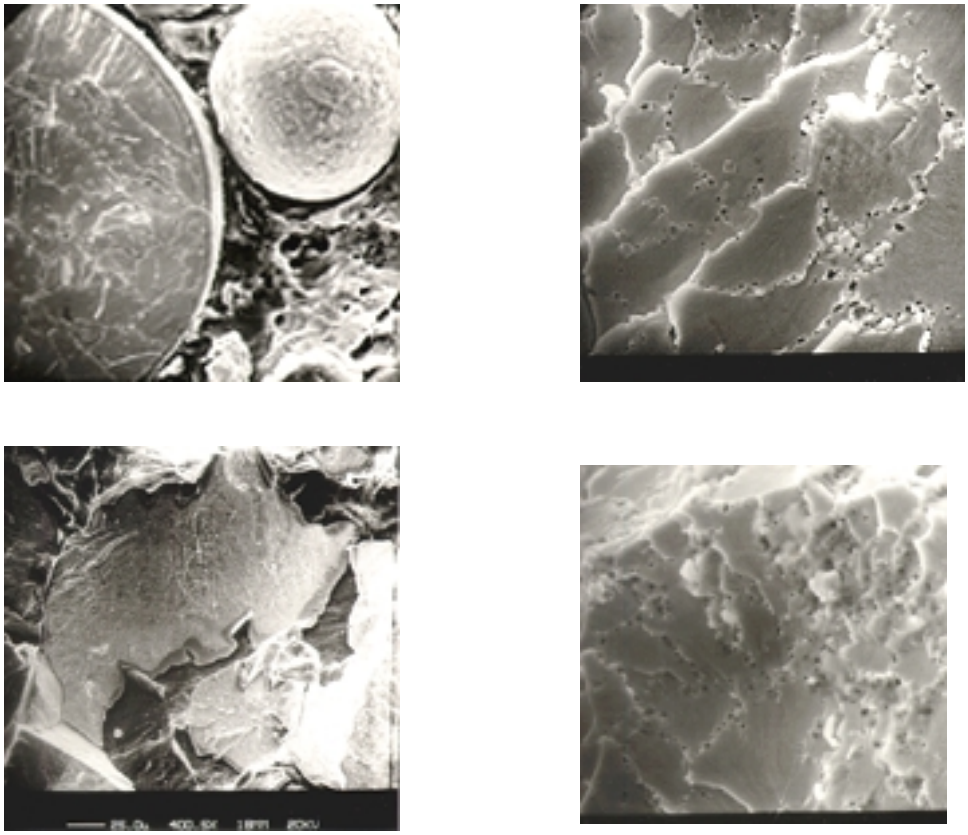

Fig. 2. SEM Fractographs of an Atomized and Machined (lower) U-10Mo Sample After ~40 at.% U-235 burnup.

The apparently fine-grain structure in many of the ground fuel particles must be considered coincidental, and results from an entirely different metallurgical process. The ground particles are obtained by machining large grained alloy rods using a rotating tungsten carbide file. In this operation the particles become heavily cold worked and contain a very high density of dislocations. Such a heavily cold worked metal may undergo recovery and recrystalization when suitably heated for a sufficient time. These conditions do indeed occur during rolling of the fuel plate samples. It is likely that owing to the variability in cold work existing in the various particles, as well as other possible variables such as tungsten contamination that was found to be present, some particles fully or partially recrystalized during rolling with a grain structure that by coincidence resembles that of atomized fuel particles. Other particles may not have fully recovered during rolling and their final dislocation structure may have contained more preferential nucleation sites for bubbles to form and grow earlier in the irradiation resulting in the more profuse bubble morphology also shown in Fig. 3. Detailed examinations of preirradiated fuel samples are being performed to illucidate the observed variable (see Fig. 4) behavior of ground fuel particles. An example of the variation in preirradiation microstructure and corresponding variable fission bubble morphology is shown in Fig. 4. The higher density alloys have not been examined in great detail to date because samples of the higher burnup RERTR-2 test became available and were given priority. Moreover, the following two examples serve to illustrate the expected behavior of the remainder of the RERTR-1 test matrix. Figure 4 shows an optical micrograph and SEM fractographs of U-6 Mo-0.6 Ru, U-6 Mo-1 Pt was also examined and found to be virtually identical. As was the case for U-10Mo, no fission gas bubbles are visible at a magnification of 500x.

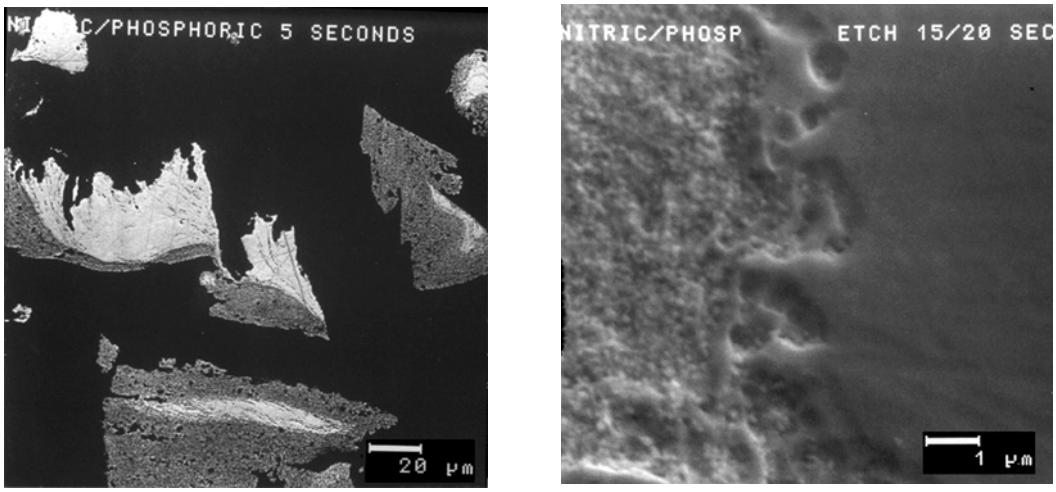


Distinction between "smooth" and "grainy" regions, pre-irradiation

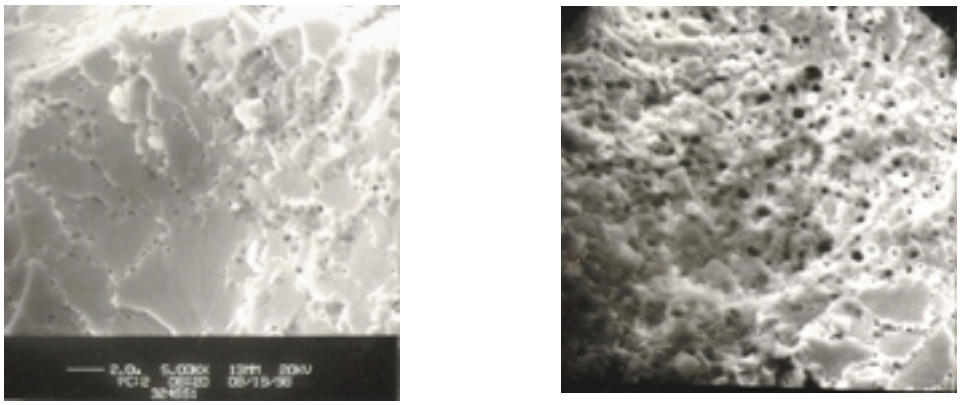

Distinction between regions of different bubble morphology

Fig. 3. Correlation of Pre- and Postirradiation Microstructure in Ground U-10Mo Fuel Particles After ~40 at.% U-235 Burnup.

The SEM fractographs of U-6 Mo-0.6 Ru (as well as U-6 Mo-1 Pt) revealed a surprising change in microstructure. The alloy has transformed into a very fine grain structure that is very similar to that earlier found in high burnup $U_3O_8$ dispersion fuel[2] and more recently in $UO_2$ power reactor fuel where it was coined "rim effect". This grain refinement is thought to be due to the accumulation of irradiation (fission) induced dislocations that eventually leads to a recrystallization of the fuel. After this occurs, the boundaries between the new small grains become favored nucleation sites for fission gas bubbles. These sites being numerous provide a favorable dispersion of a high density of small gas bubbles. Some larger bubbles appear to be associated with random patches of fuel that has not participated in the grain refinement, possibly due to the presence of impurities. It will be shown in the discussion of RERTR-2 samples that grain refinement is a general occurring phenomenon in all U-Mo fuel alloys. The last sample from RERTR-1 discussed here is U-5Mo-3Zr of which optical micrographs are shown in Fig. 5.

The difference between this fuel and the various U-Mo fuels is obvious. The fuel plate, as well as other U-Nb-Zr plates, had shown considerable swelling during fabrication indicating fuel-aluminum interaction. The very large cavities, the bubble-free parts of the fuel particles, and the large reduction of matrix aluminum are evidence of aluminide formation. The original γ-phase in these alloys is more

unstable than in U-Mo alloys of similar density. The decomposition of the γ-phase during fabrication lead to rapid interdiffusion of α-U and Al as well as rapid fission gas bubble growth in the remaining unreacted fuel during irradiation. The U-Nb-Zr alloys are clearly not suitable for high burnup, high volume loading application.

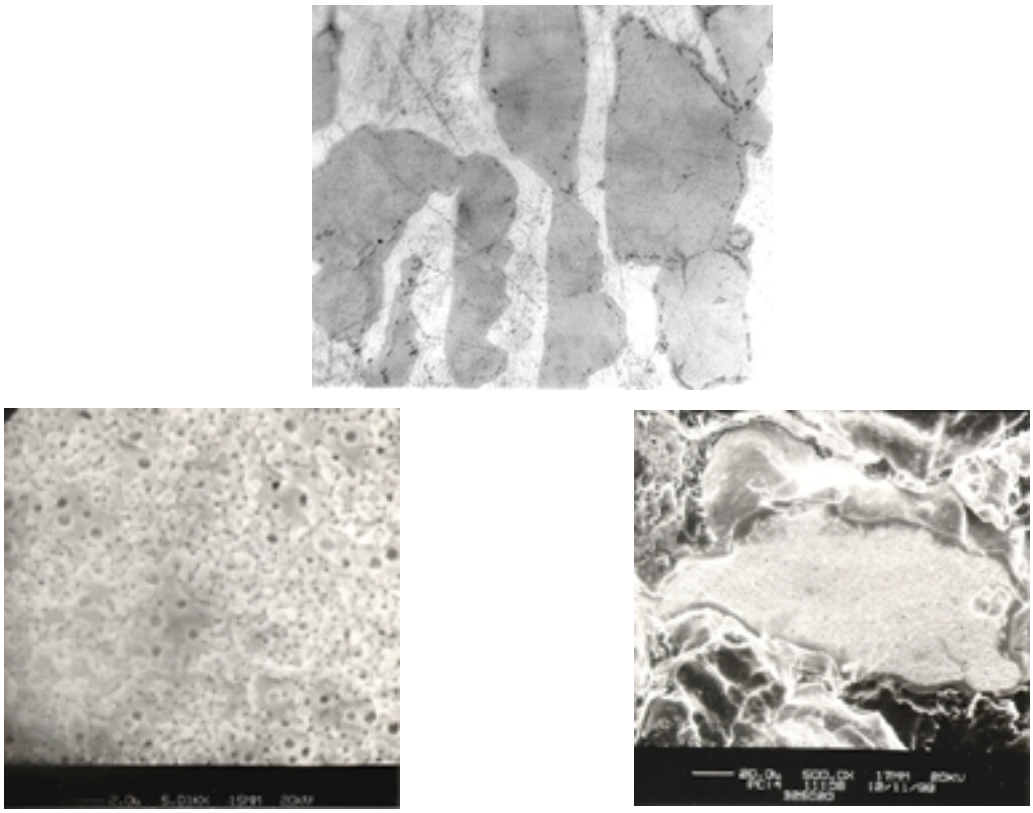

Fig. 4. As-polished cross-section and SEM fractographs of a U-6Mo-0.6Ru Sample After ~40 at.% U-235 Burnup.

#### 3.2 RERTR-2 @ ~70% U-235 Burnup

The first observation to be made on the optical micrographs of the 70% burnup samples is that fission gas bubbles are now visible at a magnification of 500x in all alloys (see Fig. 6-8). There appear to be two different populations of gas bubbles. One with an average bubble diameter of ~1 μm, and another, very dense, population with much smaller average diameters. The proportion of the former increases when the Mo content decreases and is dominant in the U-4Mo alloy. In addition, the U-4Mo alloy contains very large bubbles resembling those found in other unstable fuels. The alloys may be classified into three groups, according to fission gas bubble formation, as shown in Fig. 8.

The fuel particles in the first group, consisting of U-10Mo, U-8Mo, and U-6Mo - 0.6Ru, contains a very small fraction of the larger bubble population. This fraction is substantially larger in the second group that consists of U-6Mo-1Pt and U-6Mo. The bubble morphologies in all these five alloys indicates stable swelling behavior with no indication of bubble interlinkage and incipient breakaway swelling. This is, however, not the case for U-4Mo, which makes up the third group. Bubble coarsening and linkup clearly indicate the beginning of break away swelling. In addition, substantial fuel-Al interaction is evident, to some extent resembling that found in U-Nb-Zr shown in Fig. 6.

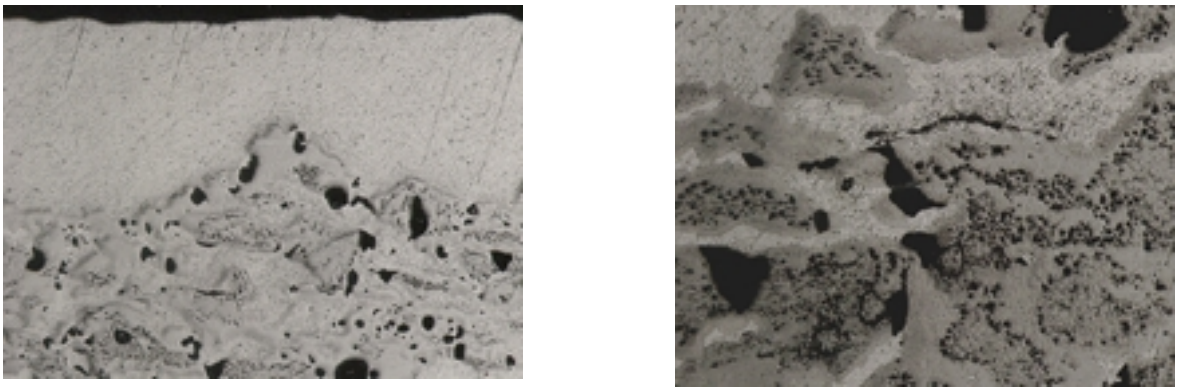

ET291979, (75X) ET291985 (250X)

Fig. 5. As-polished Cross-section of a U-5Nb-3Zr Sample After ~`40 at.% U-235 Burnup.

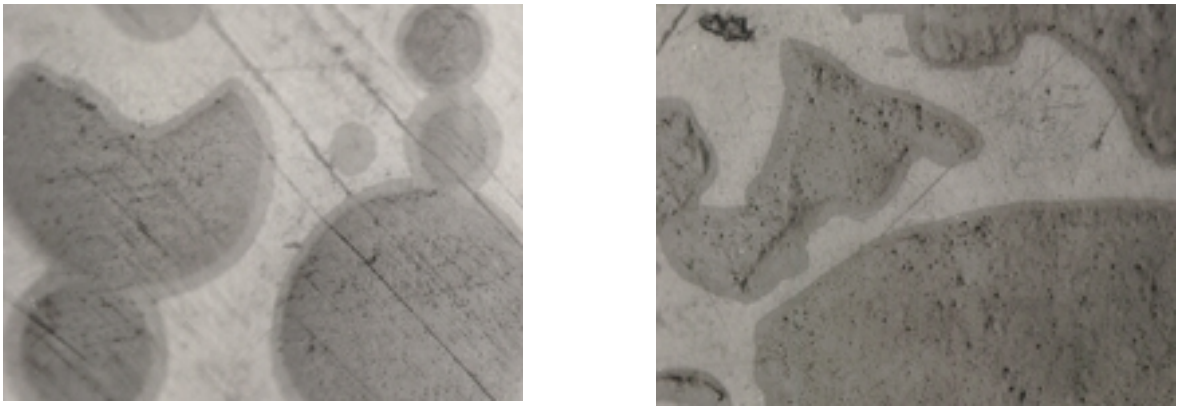

ET291931, 537Y3 (500X ET291973,557V3 (500X)

Fig. 6. As-polished Cross-section of Atom Gas and Ground U-10Mo Samples After ~70 at.% U-235 Brunup.

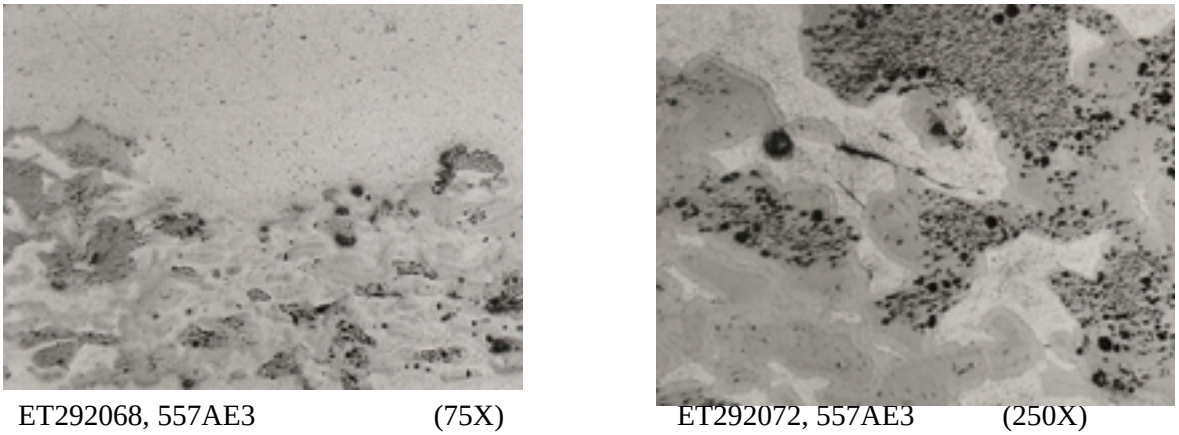

ET292068, 557AE3 (75X) ET292072, 557AE3 (250X)

Fig. 7. As-polished Cross-Section of U-4Mo Sample After ~`70 at.% U-235 Burnup.

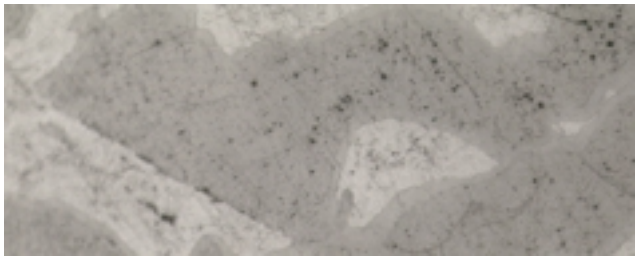

U-10Mo

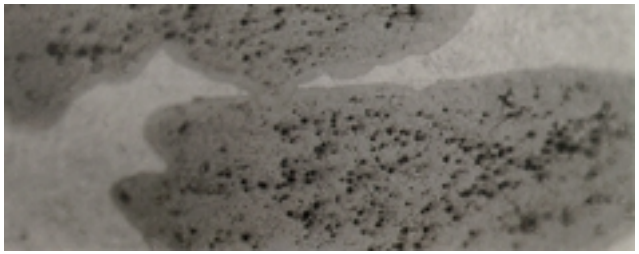

U-6Mo-1Pt

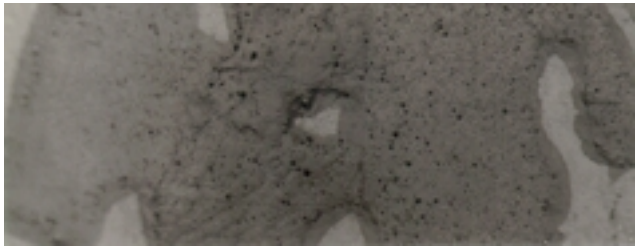

U-8Mo

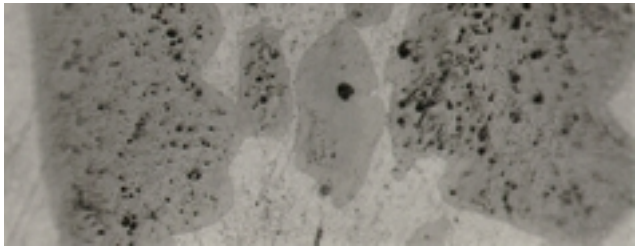

U-6Mo

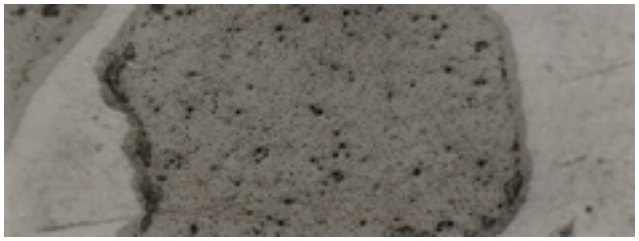

U-6Mo-0.6Ru

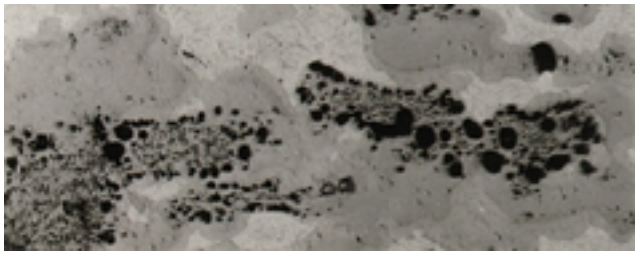

U-4Mo

Fig. 8. Comparison of Various Ground U-Mo Fuel Samples After ~70 at.% U-235 Burnup

It appears that there is a threshold between U-6Mo and U-4Mo where the fuel behavior changes from favorable to unacceptable. The underlying microstructure of the various fuel alloys is shown in Fig. 9. All fuels except U-4Mo have undergone "grain refinement", recall that this was already complete at 40% burnup for U-6Mo-Ru and U-6Mo-Pt. The U-10Mo spherical fuel, which had not shown any grain refinements at 40% burnup is still lagging somewhat in completing this transformation, presumable, as mentioned before, because of the lack of cold work in the atomized particles. Also, as discussed below, compositional segregation in the atomized fuel particles appears to have an effect.

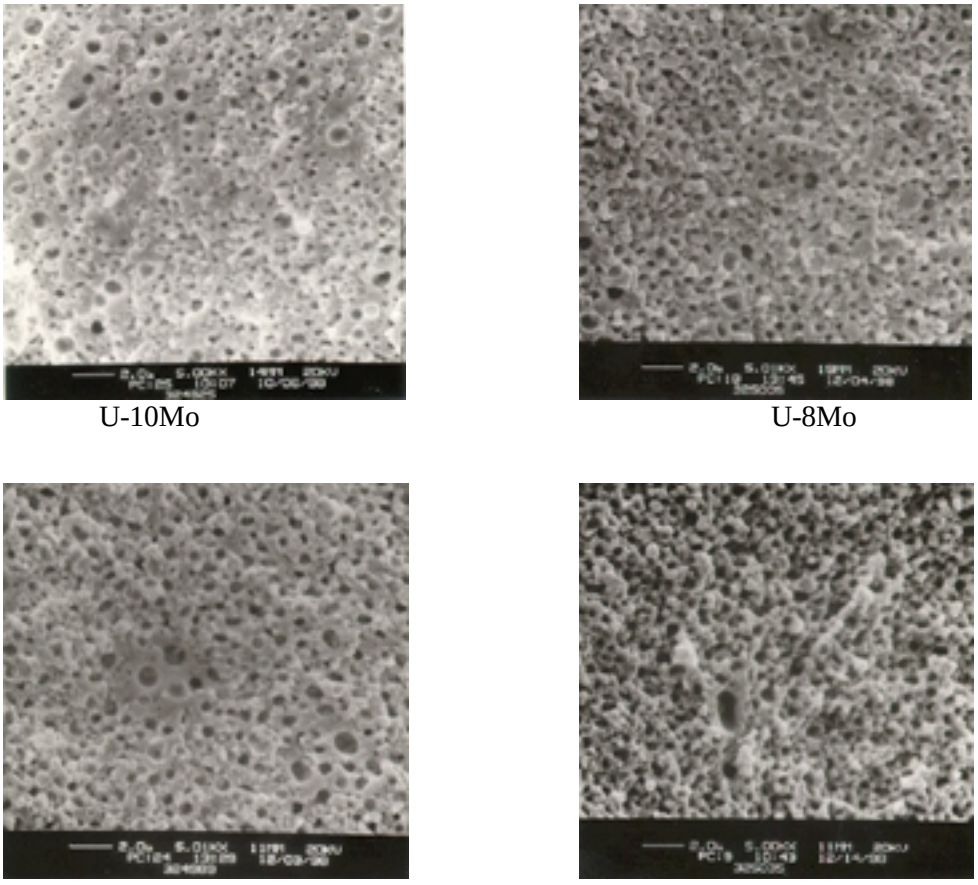

U-10Mo U-8Mo

U-6Mo-1Pt U-6Mo

Fig. 9. Fracture Surfaces of Various Ground Fuel Particles After ~70 at.% U-235 Burnup

The exception to the generally similar microstructural evolution of the alloys is U-4Mo. The behavior of this alloy may, to a large extent, be compared to that of U-Nb-Zr. During fabrication of the samples at 500°C, U-8Mo as well as U-Nb-Zr decompose from the metastable γ-phase to the equilibrium α-δ phases and reacted significantly with the matrix aluminum. The unreacted parts of the fuel particles remained in a two-phase state in which fission gas bubbles readily nucleate and grow.

Pre-irradiation X-ray diffraction showed that some decomposition of the γ-phase occurred as well in all but the U-10Mo and U-8Mo alloys, albeit to a much lesser extent. The known phenomenon of phase reversal at high fission rates[3] most likely was effective in reverting the two-phase structure back to the γ-phase in all but the thermodynamically least stable alloys, i.e., U-4Mo as U-Nb-Zr as no evidence of a two-phase structure is found in any of the well behaved alloys.

Whereas the SEM images of fracture surfaces clearly reveal the fine-grained microstructure of the various fuel alloys, they appear to exaggerate the porosity when compared to optical images. In order to characterize the true porosity at higher magnification, selected small samples were polished and examined by SEM as well. A comparison of fracture and polished surface images is shown in Fig. 10. The appearance of the larger spherical bubbles in the machined fuel particles is not affected by polishing, however, the more numerous fine pores, already visible in the optical image, are shown to be irregular and angular in shape in the SEM image. Judging from their shape and spacing, these pores are situated on junctions of boundaries between the fine grains. A similar comparison for the atomized fuel particles is shown in Fig. 11. When compared with pre-irradiation microstrucutre, it appears that the fine grain microstructure and its associated fine porosity occurs in one of the segregated γ-phases (the lower Mo) while the second (higher Mo) phase has, at this burnup of 70%, not undergone grain refinement nor visible fission gas bubble formation. The basic fission gas bubble morphology of the various U-Mo alloys is, however, very similar as shown in Fig. 12. The differences in the overall porosity, i.e., the occurrence of an additional population of larger bubbles in the machined particles, and the heterogeneous distribution of fine porosity in the atomized particles, is the result of microstructural features introduced during fabrication of the two different fuel powders.

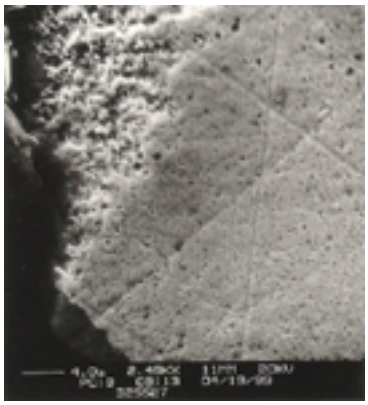

**Fracture ←as polished, SEM**

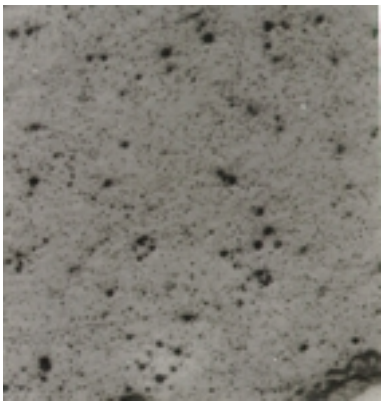

**As polished, optical**

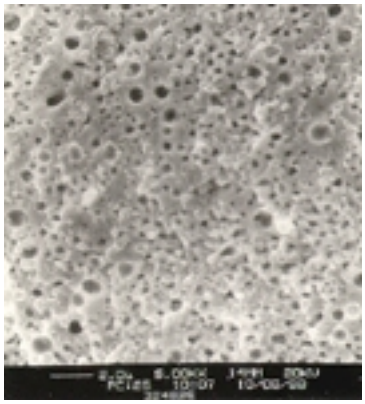

**Fracture, SEM**

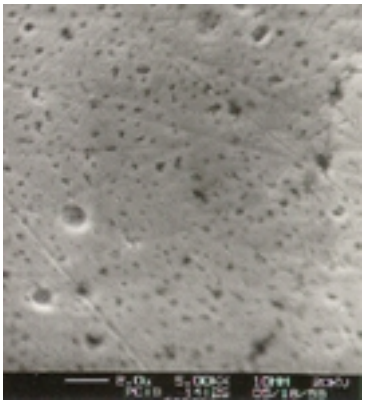

**As-polished, SEM**

**Fig. 10. Comparison of Fractured and Polished Surfaces of U-10Mo Ground Fuel Particles After ~70 at.% U-235 Burnup**

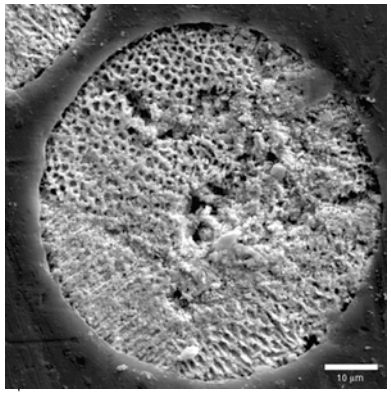

**Pre-Irradiation**

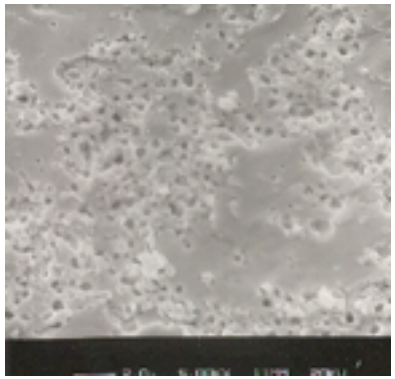

**Fractured**

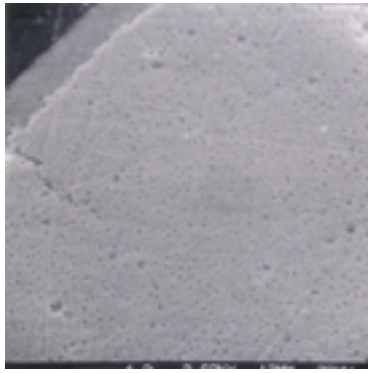

**U-10Mo, ground**

**U-10Mo Atomized**

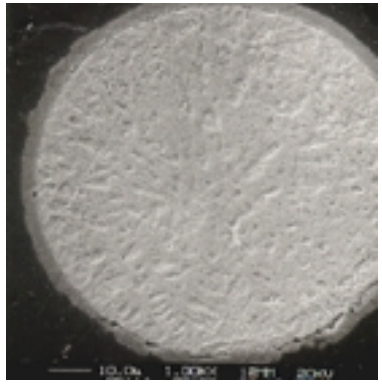

**Polished**

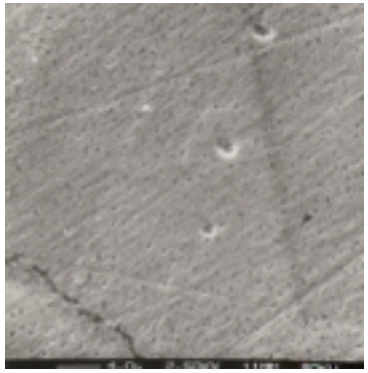

**U-6Mo, ground**

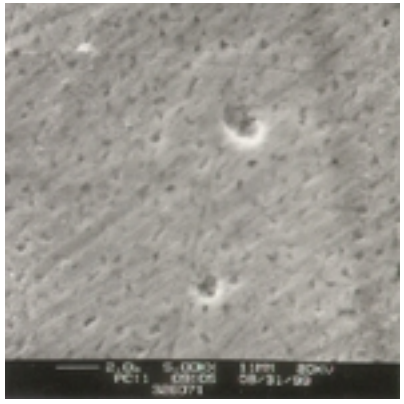

**U-6Mo, ground**

**Fig. 11. Comparison of Fractured and Polished Surfaces of Atomized U-10Mo Fuel Particles After ~70 at.% U-235 Burnup and Pre-irradiation (etched) Microstructure (SEM)**

**Fig. 12. Comparison of Bubble Morphologies on Polished Surfaces of Various Fuel Particles After ~70 at.% U-235 Burnup (SEM)**

### 4. Fuel-Aluminum Interaction

Fuel-Al interaction, in effect interdiffusion of the matrix Al and the dispersed fuel alloy, results in the formation of a layer of an intermediate phase at the particle periphery. Interdiffusion of U an Al is very rapid at temperatures above ~300°C, hence the extensive interaction of the decomposed alloys, U-4Mo and U-Nb-Zr, at the rolling temperature of 500°C. In the case of retained γ-phase alloys and uranium-silicide compounds, the interaction is negligible during the few hours of fabrication when the dispersion is maintained at 500°C.

An additional interaction occurs during irradiation even at temperatures of 100°C or less. The rate of this fission-enhanced interdiffusion is proportional to the fission rate and has a weak temperature dependence. Previous experiments have shown that in highly loaded dispersions the extent of interdiffusion may lead to complete depletion of matrix Al at temperatures of ~250°C and higher. This was found to be accompanied by excessive swelling of the dispersion. It is, therefore, important to determine the rate of interdiffusion in the present alloy fuels. The width of the interaction layer, which is clearly distinguishable in both the optical micrographs and SEM fractographs, was measured on several samples at 40 and 70% burnup. The date are shown in Fig. 13 -- a plot that contains, for comparison, earlier data from irradiations of $U_3Si_2$ and $U_3Si$ at ~100°C dispersion temperatures. A correlation of the extent of interaction with temperature, fission rate, and time was derived from these earlier silicide irradiations in the ORR.

The depth of interaction "y" thus derived may be expressed as:

$$y(\text{cm}) = \left\{ 5.07 \times 10^{-26} \, \dot{F} \exp\left[65420 / RT\right] t \right\}^{1/2}$$

where: $\dot{F}$ is the fission rate in the fuel particle in $\text{cm}^{-3}\text{s}^{-1}$ and
t is the effective full-power irradiation time in seconds.

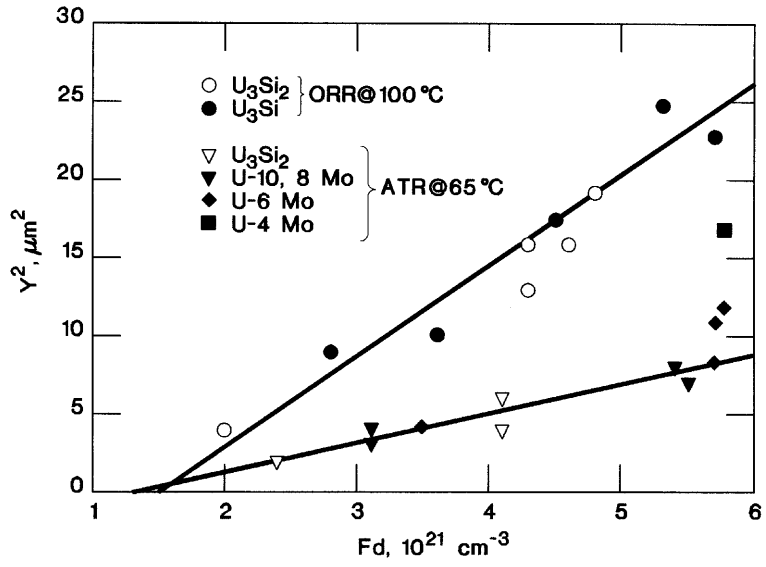


Fig. 13. Width of Fuel-Aluminum Interaction from "y" in U-Mo and $U_3Si_2$ Compared with Data and Correlatin from Previous Miniplate Irradiations

The RERTR-1 and 2 data shown in Fig. 13 can be fitted tot his equation for a temperature of 65°C. This temperature is very near the calculated value of 70°C obtained with ATR parameters. This fit and the fact that the interaction data of $U_3Si_2$ samples included in the ATR test fall on the same curve as the U-Mo data, as also shown in Fig. 13, lead us to project interaction behavior of the U-Mo alloy with at least 6 wt.5% Mo to be similar at higher temperatures.

Although the width of the interaction seen is similar for U-Mo and $U_3Si_2$, preliminary data suggests that the stoichiometry of the former is $(U_3Mo)Al_3$ whereas that of the latter is $U(Si_3Al)_3$. The formation of the interaction phase in the U-Mo alloy would therefore involve a greater amount of aluminum.

## 5. Conclusion

At low irradiation temperatures, ~70°C:

- U-Mo alloys with at least 6 wt.% Mo show low and stable swelling behavior. These alloys are very promising for further development of high-density dispersion fuels.
- Alloys with 4 wt.% Mo and U-Nb-Zr alloys signs of break-away swelling. These alloys do not warrant continued testing.
- The extent of Fuel-Al interdiffusions is similar to that seen in $U_3Si_2$-Al, although Al matrix depletion is relatively higher.
- The effect of higher temperature and U loading, is to be explored in the RERTR-III experiment, presently in the ATR.

## REFERENCES

1. M.M. Meyer, G.L. Hofman, J.L. Snelgrove, C.R. Clark, S.L. Hayes, and R.V. Strain, "Irradiation Behavior of Uranium-Molybdenum Dispersion Fuel: Fuel Performance Data from RERTR-1 and RERTR-2," presented at the 1999 International Reduced Enrichment for Research and Test Reactor Conference, Budapest, Hungary, October 4-8, 1999.

2. Gerard L. Hofman, et al, "Microscopic Investigation into the Irradiation Behavior of $U_3O_8$-Al Dispersion Fuel," *Nuclear Technology*, Vol. 2, March 1986

3. M.L. Bleiberg, "Effect of Fission Rate and Lamella Spacing Upon the Irradiation-Induced Phase Transformation of U-9 wt% Mo Alloy," *J. Nucl Mat.* **2** 182-90 (1959).S